Research paper

Influence of weak acid salts and curing condition on supersulfated cement mortar

Nguyen Khanh Son[1], Nguyen Ngoc Tri Huynh[2], Thanongsak Imjai[3], Mohd Mustafa Al Bakri Abdullah[4], Katarzyna Błoch[5]

Abstract: This study explores the impact of weak acid salt agents (citrate and tartrate) in the mixture and various curing conditions on the properties of supersulfated cement (SSC) mortar. Compressive strength tests were conducted on prism-shaped samples measuring $4 \times 4 \times 16$ cm. A comprehensive analysis of the phase assemblage of hardened products was carried out using X-ray diffraction (XRD), differential scanning calorimetry (DSC), and scanning electron microscopy (SEM) coupled with energy-dispersive X-ray spectroscopy (EDS). The results reveal the abundant formation of ettringite (E) and hydrotalcite (Ht) when weak acid salt agents are added, especially in chloride and sulfate-rich curing solutions, leading to a notable increase in compressive strength, up to 200% compared to the control sample. Furthermore, the study demonstrates a substantial improvement in early and overall strength under temperature-stimulated curing conditions, accelerating the hydration reaction of SSC. These findings provide deeper insights into the factors influencing SSC hardening and strength development, offering valuable information for enhancing the efficiency and utilization of SSC in the construction industry, aligning with the goals of sustainable development.

Keywords: supersulfated cement, GBF slag, weak acid salt agent, curing condition, durability

[1]PhD., Eng., Ho Chi Minh City University of Technology - VNU-HCM, Faculty of Materials Technology, Ho Chi Minh city, Vietnam, e-mail: ksnguyen@hcmut.edu.vn, ORCID: 0000-0002-4173-687X
[2]PhD., Eng., Ho Chi Minh City University of Technology - VNU-HCM, Faculty of Materials Technology, Ho Chi Minh city, Vietnam, e-mail: nnthuynh@hcmut.edu.vn, ORCID: 0000-0003-2085-3564
[3]Assoc. Prof., PhD., Eng., Walailak University, School of Engineering and Technology, Nakhonsithammarat, Thailand, e-mail: thanongsak.im@wu.ac.th, ORCID: 0000-0002-3220-7669
[4]Prof. PhD., Eng., Centre of Excellence Geopolymer and Green Technology (CEGeoGTech), Universiti Malaysia Perlish (UniMAP), Perlis, Malaysia, e-mail: mustafa_albakri@unimap.edu.my, ORCID: 0000-0002-9779-8586
[5]Prof., PhD., Eng., Czestochowa University of Technology, Department of Physics, Faculty of Production Engineering and Materials Technology, al. ArmiiKrajowej 19, 42-200 Częstochowa, Poland, e-mail: katarzyna.bloch@pcz.pl, ORCID: 0000-0002-5405-1845

1. Introduction

Supersulfated cement (SSC) is a specialized cementitious material that has gained attention due to its unique properties and potential applications as an alternative to ordinary Portland cement (OPC). SSC differs fundamentally from OPC in terms of its composition and performance characteristics. It typically comprises less than 5% wt Portland cement clinker and up to 95% wt of granulated blast-furnace slag (GBFS) and calcium sulfate. The history of SSC can be traced back over 100 years when it was first introduced as "gipsschlackzement" and patented by H. Kuhl in 1908. Initially composed of blast furnace slag and gypsum, this cement type was later standardized as supersulfated cement in Germany in 1937. It recorded significant production and usage from the 1940s to the 1960s, particularly in countries like Germany, Belgium, the UK, and France, coinciding with the development of the steel industry in those regions. However, the gradual decline of SSC can be attributed to concerns regarding blast furnace slag quality, compressive strength, and durability compared to ordinary Portland cement [1].

Nevertheless, SSC's notable features, such as its high resistance to sulfate solutions, peaty acids, oils, and other contaminants commonly found in wastewater and contaminated soils, were also attributed to its high slag content. Furthermore, this high slag content offers a significant advantage in reducing the carbon footprint of cement production compared to OPC [2]. Consequently, there has been a renewed interest among researchers and the industry in the production and application of SSC, exploring its distinct properties and capitalizing on its sustainability as a specialized cement suitable for the construction sector where ordinary Portland cement may not be suitable [2].

The unique properties of supersulfated cement have resulted in the development of a dedicated standard, EN 15743:2010, tailored explicitly for this specialized cement [3]. This standard distinguishes supersulfated cement from other types of Portland cement and blended Portland cement. The setting and hardening processes of SSC are fundamentally different from the well-known hydration reaction of OPC, as they rely on the subsequent alkaline activation of blast furnace slag and the combination reaction with calcium sulfate [4]. The standard emphasizes the requirements for mixing proportions and the materials' quality, with particular attention to the reactivity of slag and alumina content. These factors significantly influence the performance and characteristics of SSC [5]. Furthermore, SSC is classified into four distinct classes based on varying technical specifications, encompassing criteria such as compressive strength development, setting period, and hydration heat. These classifications provide practical guidelines for achieving desired performance and facilitate the appropriate application of SSC in construction projects.

Rising sea levels and soil contamination from industrial wastewater and agricultural waste pose challenges that contribute to the degradation of civil structures. To address these challenges, concrete materials must exhibit enhanced durability when exposed to severe conditions. Conventional concrete undergoes subsequent reactions that lead to volumetric instability when exposed to acid solutions and high sulfate concentrations [7]. This instability results in cracks and the penetration of harmful elements, causing corrosion and deterioration of reinforcement and ultimately reducing the overall lifespan of structures. With its unique properties and resistance to aggressive environments, SSC offers a promising solution to mitigate such

challenges [5]. In addition, SSC shows promise in soil stabilization applications, particularly through cement deep mixing. Soil stabilization is critical to infrastructure development, especially in areas of weak or problematic soils, such as river deltas in many cities. One of the drawbacks of using ordinary Portland cement in deep mixing is its setting behavior, which can be affected by the low pH of the soil environment [8]. By utilizing SSC, which exhibits enhanced resistance to low pH conditions, the technique of cement deep mixing can be more effectively employed for soil stabilization, improving the load-bearing capacity and stability of the soil [8]. The mechanism of the hydration reaction of SSC cement with the presence of weak acid salt agents involves the dissolution of Na^+ ions, leading to an initial rise in pH. This increase positively contributes to the easy dissolution of slag in a highly alkaline solution as detailed in the publication by Xing et al. [9].

Supersulfated cement has been observed to have certain limitations, such as prolonged setting time, low early-age strength, and susceptibility to later-stage carbonation reactions [10]. This study aims to address these challenges by examining the impact of weak acid salt additives, curing temperature, and curing solutions on the mechanical properties, microstructure, and composition of the hydration product of supersulfated cement. Such investigation allows us to enhance early-age strength, ensuring adequate strength development and long-term durability of SSC mortar. The identification of hydrated products will be carried out through materials analysis techniques. Furthermore, the mechanical resistance of prepared mortar prisms will be compared. By expanding our understanding of SSC behavior under different conditions, this research provides valuable insights for optimizing the performance and utilization of SSC-based solutions in sustainable construction practices and infrastructural development.

2. Materials and analysis

Four raw materials are utilized to formulate supersulfated cement: blast furnace slag (produced by JFE, Japan), natural gypsum, lime, and Portland cement clinker. Additionally, two weak acid salts, sodium citrate, and sodium tartrate, are employed as additives to adjust the reaction process. Among these materials, blast furnace slag is the primary component for the curing reaction and necessitates specific quality criteria, including fineness, composition, and activity. Finely ground Portland cement clinker creates an alkaline environment that aids in slag dissolution. The sulfate component facilitates the combination reaction by providing the SO_4^{2-} ions.

Table 1 presents the three starting materials along with their analysis results. The achieved fineness through grinding is crucial for the activity and solubility of the slag. Notably, the Blaine fineness measures 4270 cm^2/g, while the slag material exhibits a significant aluminum oxide content of 15.6% wt.

The X-ray diffraction (XRD) analysis spectrum indicates the prevalence of glassy and amorphous phases (Fig. 1(a)). Moreover, the particle size composition analysis, depicted in the accompanying figure, underscores that a substantial 82.13% volume of particles is below 45 μm in size (Fig. 1(b)). It is noteworthy that this aligns with the earlier Blaine result of 4270 cm²/g, indicating good fineness and contributing to the reactivity of the slag material.

Table 1. Main physio-chemical properties of slag, anhydrite and PC clinker for supersulfated cement formulating

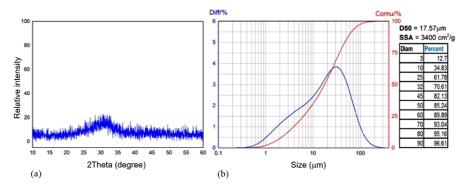|	GBF Slag	Anhydrite	PC clinker
Physical properties			
Specific density	2.91	2.32	3.17
Mean diameter, μm	30	100	32
Blaine surface area, cm^2/g	4270	2950	3740
Chemical composition (% wt)			
SiO_2	33.65	2.00	22.27
Al_2O_3	15.60	1.00	4.11
CaO	42.12	49.68	61.87
SO_3	0.16	46.27	1.18
MgO	6.40	0.16	2.21
Fe_xO_y	0.84	0.33	4.51
Others	0.17	0.78	0.17
Loss on ignition	0.56	0	0.71
Others characteristics			
Insoluble residues, % wt	0.49	–	0.48
Main mineral phases	Amorphous	$CaSO_4$	45.2% wt C_3S; 29.7% wt C_2S; 3.2% wt C_3A; 13.7% wt C_4AF;
Strength activity index 28 days, %	110	–	–

Fig. 1. (a) Spectrum of XRD analysis of JFE's origin slag materials; (b) Particle size distribution of slag powder

3. Formulation of SSC and experiments

According to standard definition, the proportion mixture of supersulfated cement typically consists of ⩾ 75% wt granulated blast-furnace slag (GBFS), 5–20% wt anhydrite, ⩽ 5% wt Portland cement clinker and/or hydrate lime [3]. These powdered materials are thoroughly mixed using shear mixer equipment with five cutting blades in a star-shaped configuration. The barrel rotates at 50 rpm, while the blades rotate at 400 rpm in an inverse direction. Following the mixing process, the resulting mixture is tightly stored in a zipper bag to prevent moisture absorption before conducting experiments and analyzing the specific characteristics of the cement. Regarding diverse formulations, we conducted tests with two compositions, namely 78% and 80% by weight of slag, with a focus on their potential applications in soil mixing and SSC concrete. The detailed compositions of the materials and the corresponding curing conditions are summarized in Table 2.

Table 2. Formulation of SSC and specific curing conditions

List	Formulation of SSC (% wt)			Weak acid salts (%wt of solid)	Curing condition
	GBF slag	Anhydrite	PC clinker		
1	78	17	5	–	$T = 27°C$, RH = 95%
2				Sodium Citrate 0.1, 0.2, 0.5	$T = 27°C$, RH = 95%
3				Sodium Tartrate 0.1, 0.2, 0.5	$T = 27°C$, RH = 95%
4	80	15	5	–	Stage 1: at $T = 30°C/ 50°C/ 60°C/ 70°C$, RH = 100% during 24 hours Stage 2: cured at $T = 27°C$, RH = 95% during 27 days
5				–	at $T = 27°C$, in tap water / NaCl / NaCl + Na_2SO_4 solution (RH = 100%)

For the specific tests, two categories of specimens were prepared. In the case of material analysis, cube-shaped paste samples measuring $1 \times 1 \times 1$ cm were produced by mixing the prepared SSC with tap water at a water-to-cement ratio (W/C) of 1/1. For the compressive strength test, prism-shaped mortar samples measuring $4 \times 4 \times 16$ cm were cast by mixing the prepared SSC with tap water and standard sand at a water-to-cement-to-sand (W/C/S) ratio of 0.5/1/3. These salts were pre-dissolved separately in tap water when incorporating weak acid salts. It should be noted that the high content of fine particles in the slag may affect the consistency of the mixture. Therefore, a deep mixing approach was adopted in the planetary mixer for 6 minutes. This method allows for the release of any trapped water within the solid particles and ensures a homogeneous mixture. It is important to mention that one of the limitations in the application of supersulfated cement is its lower ductility compared to Portland cement [6]. After demolding, the hardened samples were cured for a duration of 28 days. As indicated in Table 2, three types of curing solutions were utilized: NaCl solution at

a concentration of 3.0% wt, a mixture of NaCl at a concentration of 3.0% wt, and Na_2SO_4 at a concentration of 2.0% wt (simulated seawater). Additionally, some samples were first subjected to different temperature conditions for 24 hours, such as room temperature (30°C), 50, 60, and 70°C then placed in the moisture condition of the curing tank.

Various material analysis techniques were utilized to characterize the cement paste's hydrated products. These techniques included X-ray diffraction (XRD, Bruker D8 ADVANCE), Differential scanning calorimetric (DSC, Labsys Evo TG/DSC 1600°C), and scanning electron microscopy with energy-dispersive X-ray spectroscopy (SEM/EDS, Hitachi S-4800). Furthermore, to assess the compressive strength of the hardened cement mortar, tests were carried out by the guidelines of the Vietnamese standard TCVN 6016:2011 (in line with the European standard EN 196).

4. Results and discussion

4.1. Effect of the different mixing agents of weak acid salt (sodium citrate 0.1, 0.2, 0.5% wt / sodium tartrate 0.1, 0.2, 0.5% wt)

Figure 2 illustrates the pH value changes when incorporating weak acid salts into SSC cement. Sodium citrate and sodium tartrate were used at varying dosages of 0.1%, 0.2%, and 0.5% by weight of cement. The pH value of the cement paste initially increased after mixing weak acid salts with SSC, compared to the control sample of SSC without additives. Over the 14-day period, the results consistently show variations for both types of weak acid salts, characterized by three distinct stages: (1) a gradual increase in pH value to its maximum peak from day 0 to day 1, (2) a gradual decrease in pH value from day 1 to day 7, and (3) a slight increase in pH value from day 7 to day 14.

In Figure 2, the pH value gradually decreased from day 1 to day 7 due to the combination reaction between dissolved slag and sulfates. Notably, with 0.5%wt of weak acid salt, the pH value decreases faster after only 3 days instead of 7 days. This result suggests that the stimulated mineralization reaction occurs more rapidly when using a higher additive dosage. Finally, the pH value stabilizes or slightly increases from day 7 to day 14. This stabilization process ensures the non-phase transition of newly formed ettringite minerals, contributing to the stability and durability of the hardened paste of supersulfated cement.

The results of compressive strength development are depicted in Fig. 3, illustrating the changes in compressive strength values for both the control sample of SSC cement and the mortar sample mixed with weak acid salts. In all cases, the compressive strength gradually increases over time as a natural consequence of the hardening process.

However, the rate of strength development and the strength values of 28-day-old curing mortar samples were significantly improved using weak acid salt additives. Specifically, when compared with the control sample of SSC that reached 23.0 ± 0.46 MPa after 28 days, the samples incorporating 0.5% wt of citrate and tartrate salt additives achieved strengths of 51.4 ± 0.65 MPa and 54.2 ± 0.36 MPa, respectively, corresponding to an increase of over 200%. This remarkable improvement in strength aligns with the previously mentioned role of weak
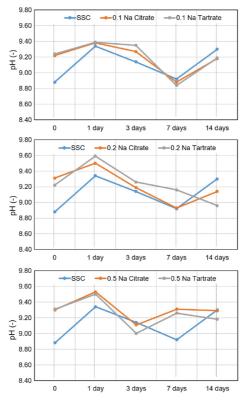
Fig. 2. Variation of pH with the presence of weak acid salt agent in SSC mixture

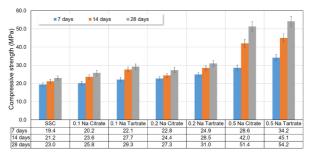|	SSC	0.1 Na Citrate	0.1 Na Tartrate	0.2 Na Citrate	0.2 Na Tartrate	0.5 Na Citrate	0.5 Na Tartrate
7 days	19.4	20.2	22.1	22.8	24.9	28.6	34.2
14 days	21.2	23.6	27.7	24.4	28.5	42.0	45.1
28 days	23.0	25.8	29.3	27.3	31.0	51.4	54.2

Fig. 3. Development of compressive strength at the age of 7-14-28 days of SSC cement mortar

acid salt additives. Stimulating the slag's initial dissolution and stabilizing the pH contributes to forming primary minerals, such as ettringite and hydrotalcite. Stabilizing these minerals is crucial, as the instability in the phase transition of these minerals has been identified as the main reason for the lower strength development of SSC cement compared to Portland cement, which possesses a more stable crystallized C–S–H structure. The results underscore the significance of weak acid salt additives in enhancing the strength development and performance of SSC cement.

Figure 4 presents SEM images of 28-day-old curing mortar samples at magnifications of ×5,000 and ×20,000. The microstructure of the hardened cement components appears compact in general.

At the same magnification, the SEM images reveal densely interlaced ettringite minerals (rod-shaped crystals) in the case of the mixture with citrate and tartrate salts (Fig. 4 – centre, right). In contrast, the control sample of SSC (Fig. 4 – left) exhibits more clearly defined plate-shaped positions of slag particles with sizes ranging from 5 to 15 μm. This contrast allows us to identify the activation character and slag dissolution process facilitated by weak acid salt additives. Additionally, the estimated results of elemental composition in two regions of the SEM images (corresponding to plate-shaped and rod-shaped mineral morphologies) indicate a higher Ca/Si ratio (Fig. 5) or crystallized calcium silicate. This provides evidence of the favorable hydration reaction in the product composition resulting from the incorporation of weak acid salt additives.
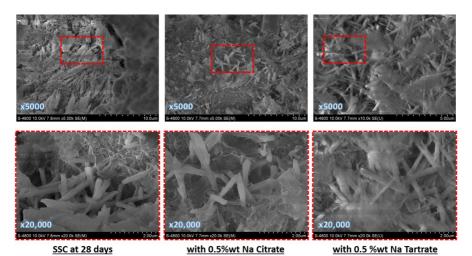

SSC at 28 days   **with 0.5%wt Na Citrate**   **with 0.5 %wt Na Tartrate**

Fig. 4. Result of SEM analysis of hardened mortar of supersulfated cement mixed with citrate and tartrate salts

Element	Ca	Al	S	Cl	Si	Mg
Weight (%)	18.32	4.18	4.27	0.77	8.75	1.96
Atomic (%)	9.14	3.09	2.66	0.43	6.23	1.61

Element	Ca	Al	S	Cl	Si	Mg
Weight (%)	25.45	4.40	4.43	2.06	9.30	1.94
Atomic (%)	13.63	3.50	2.96	1.24	7.11	1.71

Fig. 5. Result of elemental composition by SEM/ EDS analysis of hydrated supersulfated cement

4.2. Effect of the different temperature conditions of SSC curing (room temperature #30°C/ 50°C/ 60°C/ 70°C)

Figure 6 presents the mineralogical composition of hardened paste of supersulfated cement under curing temperatures of 70°C (during 24 hours), as well as the control sample of SSC. The major mineral peaks, including ettringite (E, ICSD # 16045), Friedel's salt (F, ICSD #51890), Hydrotalcite (Ht, ICSD #81963), Calcium silicat (Cs, ICSD #963) and other phase minerals from the raw materials, are prominently observed such as Gypsum (G, ICSD #2057), Anhydrite (A, ICSD #16382), Calcite (C, ICSD #52151). These peaks represent the hydration products of the slag, ensuring the curing process of the SSC cement paste and contributing to its microstructural strength. Notably, the ettringite mineral plays a vital role and is the main mineral peak on the spectrum at both 3 and 28-day-old curing paste of supersulfated cement. Comparing the age and stimulated temperature of cement curing conditions, no significant differences were observed in the categories or intensities of the peaks. This suggests that the degradation of ettringite mineral over time did not occur, regardless of whether the samples were subjected to moist thermal stimulation within 24 hours after demolding or not. The stability of ettringite mineral content is crucial for maintaining the long-term strength and durability of supersulfated cement under different curing conditions.

Two cement paste samples were analyzed using differential scanning calorimetry (DSC). One sample was subjected to temperature-stimulated curing, as shown in Fig. 7-right, while the other was not subjected to this treatment, as shown in Fig. 7-left. The DSC results revealed
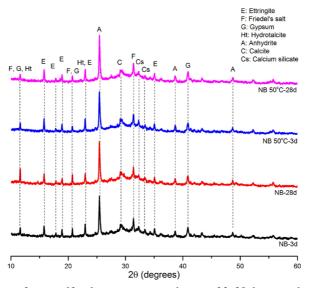

Fig. 6. XRD spectrum of supersulfated cement paste at the age of 3–28 days cured at room temperature and at 70°C during 24 hours; Mineral peaks including ettringite (E, ICSD # 16045), Friedel's salt (F, ICSD #51890), Hydrotalcite (Ht, ICSD #81963), Calcium silicat (Cs, ICSD #963) and other phase of raw materials Gypsum (G, ICSD #2057), Anhydrite (A, ICSD #16382), Calcite (C, ICSD #52151)

two main endothermic peaks corresponding to the thermal decomposition of two major phases, ettringite, and hydrotalcite, at temperatures #149°C (peak 1) and #202°C (peak 2), respectively. Notably, peak 1, associated with ettringite dehydration, plays a more significant role, considering its higher endothermal impact compared to peak 2. The XRD analysis results provided additional insights, indicating the presence of unreacted gypsum from the raw material component, in addition to the resulting ettringite mineral. As shown in Figure 7, these phases were represented by a double peak expression, suggesting consecutive dehydration reactions of gypsum and ettringite in the temperature range of 100–200°C.

A comparison between the two samples revealed that the reactions occurred earlier in the control SSC sample under the same analysis conditions than in the temperature-stimulated curing sample (at 70°C for 24 hours). Furthermore, the total enthalpy value (integration area of peak 1) of the temperature-stimulated curing sample was higher than that of the control samples. This indicates a more significant amount of ettringite phase resulting from applying temperature curing conditions. Consequently, the substantial formation of ettringite contributes to the overall strength and stability of the microstructure of the hardened SSC.

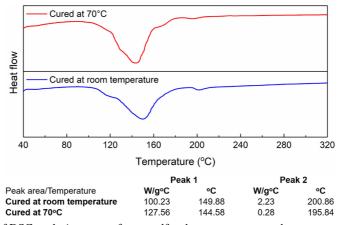| Peak area/Temperature	Peak 1		Peak 2	
	W/g°C	°C	W/g°C	°C
Cured at room temperature	100.23	149.88	2.23	200.86
Cured at 70°C	127.56	144.58	0.28	195.84

Fig. 7. Results of DSC analysis curves of supersulfated cement paste cured at room temperature and at 70°C during 24 hours

Figure 8 presents the graph of compressive strength development over the curing period for supersulfated cement mortar samples. It is evident that the strength values increased gradually with curing time, reaching the final strength at 28 days. However, when compared to the control sample, the temperature-stimulated curing sample exhibited superior strength values of 26.1 ± 0.52 MPa (cured at 60°C for 24 hours) and 27.4 ± 0.60 MPa (cured at 70°C for 24 hours), as opposed to 24.9 ± 0.64 MPa in the control. Additionally, the rate of strength increase was more pronounced at an earlier stage, starting at 3 days of age, with only slight increments at 7 and 28 days of age. The observed phenomenon can be credited to the influence of the early temperature curing conditions on the supersulfated cement mortar hardening process. The elevated temperature accelerated the hydration reaction and promoted the formation of key hydrated mineral phases (ettringite E, hydrotalcite Ht), resulting in early strength development and higher overall strength for the temperature-stimulated curing sample.
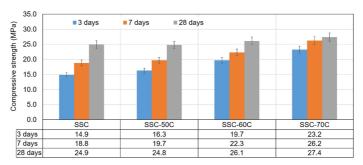
Fig. 8. Strength development at the age of 3–7–28 days of SSC cement mortar with different temperature conditions 50°C, 60° C and 70°C

4.3. Effect of the different ion solutions of SSC curing (tap water / NaCl 3% wt / NaCl 3% wt + Na$_2$SO$_4$ 2% wt)

The XRD spectra of the hydrated cement paste after 7 and 56 days of curing time are presented in Fig. 9. The major peaks observed in the spectrum correspond to the main mineral phases, including ettringite (E, ICSD # 16045), Hydrotalcite (Ht, ICSD #81963), Calcium silicate (Cs, ICSD #963), Calcite (ICSD #52151), Friedel's salt (F, ICSD #51890), gypsum (G, ICSD #2057), and anhydrite (A, ICSD #16382). Additionally, some remaining slag and/or poorly crystallized phases may contribute to the amorphous background of the spectrum. Among the hydrated minerals, ettringite appears to be the most significant phase of the cement hydration product. Some authors have characterized it as a low-Ca-ettringite product [10] compared to the high-Ca-ettringite found in Portland cement hydration products. Evidence of Friedel's salt (F, ICSD #51890) and/or hydrotalcite (Ht, ICSD #81963) phases (minor peaks at $2\theta = 11.6°$) is clearly observed in the presence of a chloride-rich solution (NaCl 3%wt) at an early age (7 days). The impact of different curing solutions must consider the role of rich sulfate ions in the solution (NaCl 3% wt + Na$_2$SO$_4$ 2% wt). This high sulfate solution favors ettringite formation at both early and later ages (7 and 56 days).

Figure 10 presents SEM images (at magnifications x10,000 and x20,000) of the hardened mortar at 7 and 56 days of curing time. The microstructure reveals the high compactness of crystallized minerals. No major cracks are observed at a magnification of x10,000, typically caused by shrinkage (plastic and thermal) of the cement paste. The morphology of the ettringite (E, ICSD # 16045) phase is identified as rod-shaped crystals. Ettringite is the dominant phase in all solutions at both 7 and 56 days of age. Some small plate-shaped particles (bright color) of the remaining slag are also highlighted. Friedel's salt (F, ICSD #81963) morphology appears as white flake crystals, as noted in the SEM images. A high density of the ettringite phase is observed in the curing solution rich in sulfate ions (NaCl 3% wt + Na$_2$SO$_4$ 2% wt), consistent with the above XRD analysis results.

Based on the SEM/EDS analysis results, it is evident that the Ca:Al ratio is approximately 3:1, which indicates the formation of C–A–H (calcium aluminum hydrates) as precursor products, contributing to the subsequent formation of ettringite (E, ICSD #16045) and Friedel's salt
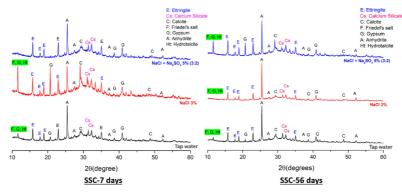
Fig. 9. XRD spectrum of supersulfated cement paste at the age of 7 and 56 days cured in different ion solutions; Mineral peaks including ettringite (E, ICSD # 16045), Friedel's salt (F, ICSD #51890), Hydrotalcite (Ht, ICSD #81963), Calcium silicat (Cs, ICSD #963) and other phase of raw materials Gypsum (ICSD #2057), Anhydrite (ICSD #16382), Calcite (ICSD #52151)
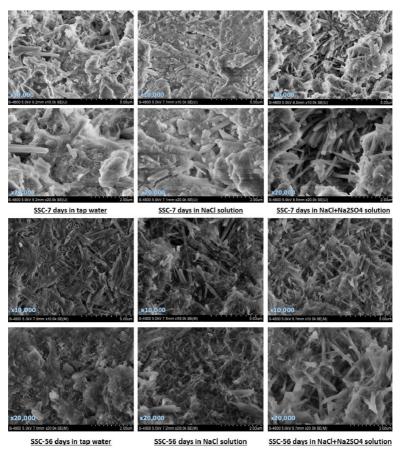

Fig. 10. Result of SEM analysis of supersulfated cement mortar at the age of 7 and 56 days cured in different ion solutions

(reaction: $Al_2O_3 + 2Cl^- + 4Ca^{2+} + 7H_2O \rightarrow C_3A \cdot CaCl_2 \cdot 10H_2O$). The presence of Cl and S elements, alongside Ca and Al, in varying proportions suggests that the surrounding environmental conditions influence the resulting mineral products.

The distinct variations in reaction products are evident from the almost negligible Cl content in the tap water curing environment. This signifies the effective binding of free chloride ions in the hydration product components of supersulfated cement when exposed to a chloride-rich environment, as highlighted by Nguyen et al. [11]. Plate-shaped positions (bright color, Fig. 11-left) on the SEM image, exhibiting high S content, indicate unreacted slag. The rod-shaped crystal positions, characterized by high Al and Si content, suggest that ettringite forms effectively in the rich sulfate ion solution, thereby enhancing the strength development. In all three curing solutions, no trace of carbon element is observed, indicating the good reactivity of SSC and its resistance to carbonation during the curing process in high-moisture solutions.

Element	Ca	Al	S	Cl	Si
Weight (%)	23.93	2.80	5.20	0	6.91
Atomic (%)	11.15	1.93	3.03	0	4.60

SSC-56 days in tap water

Element	Ca	Al	S	Cl	Si
Weight (%)	19.66	4.14	5.25	1.26	8.43
Atomic (%)	10.08	3.16	3.36	0.73	6.17

SSC-56 days in NaCl solution

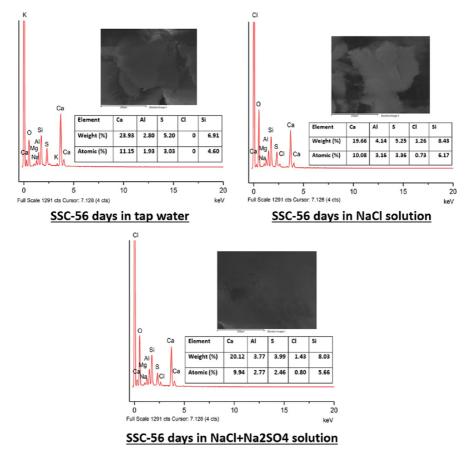| Element	Ca	Al	S	Cl	Si
Weight (%)	20.12	3.77	3.99	1.43	8.03
Atomic (%)	9.94	2.77	2.46	0.80	5.66

SSC-56 days in NaCl+Na2SO4 solution

Fig. 11. Estimation of elemental composition by using SEM/EDS analysis of supersulfated cement mortar at the age of 56 days cured in different ion solutions

5. Conclusions

In conclusion, the study on the effect of weak acid salt additives, curing temperature, and ion solutions on the physico-chemical and mechanical properties of supersulfated cement (SSC) yielded several significant findings:

– Including weak acid salt additives, such as citrate and tartrate, led to a substantial improvement in the strength development of SSC mortar samples. Adding 0.5%wt of these additives resulted in strength increases of up to 200% compared to the control sample. The elevated pH level, resulting from the inclusion of weak acid salts in the cement mixture, facilitated the dissolution of slag and promoted the formation of crucial mineral phases in a highly alkaline environment.

– Curing the samples at higher temperatures (60°C and 70°C) also resulted in superior strength to the control samples cured at ambient temperature. The early strength gain observed at 3 days of age in the temperature-stimulated curing samples demonstrated the effectiveness of high-temperature curing conditions in accelerating hydration reactions and enhancing the formation of structural phase components (ettringite, hydrotalcite). This led to the improved early and overall strength of the hardened SSC.

– The choice of different curing solutions influenced the composition of the hydration product. In chloride-rich environments, effective fixation of chloride ions in the supersulfated cement hydration product was observed, indicating enhanced resistance to chloride attack. On the other hand, high sulfate ions in the curing solution favored ettringite formation, contributing to the overall strength and stability of the microstructure in hardened SSC.

For future investigations, the aforementioned findings provide valuable insights into the optimization of SSC-based solutions. The promising compatibility of SSC with weak acid salts positions it as a potential alternative for cement deep mixing with acidic soil. Extending the study through a combination of SSC and soil, both in laboratory-scale and field-scale settings, is essential for pursuing this direction. Utilizing thermal curing and ion-rich solution curing could enhance both mechanical strength and corrosion resistance in precast concrete, particularly for civil and marine structures. Further experimental scaling to explore the potential application of SSC concrete in larger-scale deterioration processes is recommended.

Acknowledgements

References

[1] D.W. Lewis, "History of Slag Cements", presented at Symposium on Slag Cement, University of Alabama, Birmingham, 1981, pp. 1–9.

[2] A. Phelipot-Mardelé, S. Gabriel, and C. Lanos, "Super sulfated cement: formulation and uses", in *Proceedings of the Fifth International Conference on Construction Materials: Performance, Innovations and Structural Implications, CONMAT'15, Whistler, Canada 19-21 August 2015*. 2015, pp. 19–21.

[3] BS-EN 15743:2010 Supersulfated cement - Composition, specifications and conformity criteria. 2010.

[4] T. Matschei, F. Bellmann, and J. Stark, "Hydration behaviour of sulphate-activated slag cements", *Advances in Cement Research*, vol. 17, no. 4, pp. 167–178, 2005, doi: 10.1680/adcr.2005.17.4.167.

[5] O.R. Ogirigbo, "Influence of slag composition and temperature on the hydration and performance of slag blends in chloride environments", PhD thesis, University of Leeds, UL, 2016.

[6] M. Cyr and L. Andre, "Synergic effects of activation routes of ground granulated blast-furnace slag (GGBS) used in the precast industry", in *Lecture Notes in Civil Engineering, vol. 8: Proceedings of the 4th Congrès International de Géotechnique-Ouvrages-Structures: CIGOS 2017, 26–28 October 2017, Ho Chinh Minh city, Vietnam*, H. H. Tran-Nguyen, et al., Eds. Springer, 2018, pp. 588–597, doi: 10.1007/978-981-10-6713-6_58.

[7] K. Kłos, G. Adamczewski, P. Woyciechowski, and P. Łukowski, "Carbonation of concrete cover of reinforcement as a cause of loss of durability of structures", *Archives of Civil Engineering*, vol. 69, no. 1, pp. 119–129, 2023, doi: 10.24425/ace.2023.144163.

[8] A. Guimond-Barrett, "Influence of mixing and curing conditions on the characteristics and durability of soils stabilised by deep mixing", PhD thesis, Université du Havre, 2013.

[9] J. Xing, Y. Zhou, Z. Peng, J. Wang, Y. Jinm, and M. Jin, "The influence of different kinds of weak acid salts on the macro-performance, micro-structure, and hydration mechanism of the supersulfated cement", *Journal of Building Engineering*, vol. 66, art. no. 105937, 2023, doi: 10.1016/j.jobe.2023.105937.

[10] A. Gruskovnjak, B. Lothenbach, F. Winnefeld, R. Figi, S.C. Ko, M. Adlerm, and U.Mäder, "Hydration mechanisms of super sulphated slag cement", *Cement and Concrete Research*, vol. 38, no. 7, pp. 983–992, 2008, doi: 10.1016/j.cemconres.2008.03.004.

[11] K. S. Nguyen, et al., "Chloride Binding Ability and Anti-corrosion Properties of Supersulfated Cement in Seawater/Sand Mixing Concrete", in *Lecture Notes in Civil Engineering, vol. 8: Proceedings of the 4th Congrès International de Géotechnique-Ouvrages-Structures: CIGOS 2017, 26-28 October 2017, Ho Chinh Minh city, Vietnam*, H. H. Tran-Nguyen, et al., Eds. Springer, 2018, pp. 367–376, doi: 10.1007/978-981-10-6713-6_36.